Molecular Dynamics Simulations Reveal Fundamental Role of Water As Factor Determining Affinity of Binding of β-Blocker Nebivolol to β_2-Adrenergic Receptor

Karol Kaszuba,[†,‡] Tomasz Róg,[*,†] Krzysztof Bryl,[‡] Ilpo Vattulainen,[†,§,∥] and Mikko Karttunen[⊥]

Department of Physics, Tampere University of Technology, Tampere, Finland, Department of Physics and Biophysics, University of Warmia and Mazury, Olsztyn, Poland, University of Southern Denmark, Odensee, Denmark, Department of Applied Physics, Aalto University School of Science and Technology, Aalto, Finland, and Department of Applied Mathematics, The University of Western Ontario, London (ON), Canada

Received: October 18, 2009; Revised Manuscript Received: May 20, 2010

The β-adrenergic antagonists (β-blockers) constitute a class of drugs that have well-established roles in treatments of various cardiovascular diseases. Despite a 50 year history, there are two clinically important subtypes of β-adrenergic receptors (βARs) called β_1AR and β_2AR that still are promising drug targets. Our study maps the interactions between nebivolol—one of the most efficient β-blocking agents—and the β_2-adrenergic receptor by simulating two optical isomers of nebivolol: ssss-nebivolol and srrr-nebivolol. The srrr-configuration binds preferentially to β_1AR and β_2AR. The ssss-form has much lower binding affinity to both of them. Our work indicates that water is a very important component of the binding site of the β_2AR receptor. We found that the higher stereoselectivity of the srrr-configuration is due to interactions with water molecules, which extensively hydrate the binding site of β_2AR. By lowering the energy of binding, water enhanced the affinity of the srrr-form to β_2AR. We also address the problem of β_1AR/β_2AR selectivity. At higher concentrations, all β-blocking agents lose their specificity and bind nonselectively, causing many adverse effects. Our simulations indicate that PHE194, TYR308, and ILE309 of the β_2AR and the corresponding residues of the β_1AR receptor may be important determinants of β_1AR versus β_2AR selectivity.

Introduction

Receptors are membrane-embedded protein molecules onto which other, usually very few and well-defined, molecules may attach. A molecule that can bind to a receptor is called a ligand. Ligand binding induces conformational changes in the receptor that typically lead to intra- or intercellular signaling and/or other biological activity. Peptides and hormones are typical ligands. Receptors may also bind drugs and toxins, and are thus common targets for drugs. Ligands that cause biological activity on binding are called agonists. Ligands that bind to receptors without inducing any biological activity are called blockers or antagonists; they block the receptor without allowing it to become biologically active.

β-Adrenergic receptors (βARs) belong to the family of G-protein coupled receptors (GPCRs).[1,2] There are three different β-receptors called β_1AR, β_2AR, and β_3AR. The activity of β_1AR is typically related to an increase of cardiac muscle contractility and hence to an increase in cardiac output. β_1AR receptors are mostly found in the heart and kidneys. Selective β_1AR antagonists are used in the treatment of cardiac arrhythmias, congestive heart failure (CHF), and hypertension.[4,5]

β_2AR receptor activity induces smooth muscle relaxation.[1,3] As β_2AR receptors are mostly located in lungs, β_2AR agonists are commonly used in asthma inhalers.[3] Of the three β-receptors, β_3AR currently has no pharmacological importance, although there are indications that this may change. β_3AR receptors are located in adipose tissue, and their activity is related to lipolysis.[3]

Pharmacologically relevant β-blockers are often divided into two classes:[1] selective and nonselective. Nonselective β-blockers block β_1AR and β_2AR equally. Selectivity is related to β_1AR only, but administration in higher doses may cause nonselective binding to both subtypes.[1] Selective blocking of β_1AR can be advantageous in patients with bronchospastic diseases and/or peripheral vascular disease since unblocked β_2AR mediates adrenergic bronchodilation and vasodilatation;[1] administration of β_1AR selective agents lowers the risk of bronchospasm and, to a smaller extent, influences peripheral blood flow. Selective blocking of β_1AR may also have a protective effect during human heart failure[6] since sustained β_1AR stimulation induces myocyte hypertrophy and apoptosis.

Despite the benefits of β_1AR-selective blockade, the selectivity of binding remains poorly understood. The recently crystallized structures of β_1AR[7] and β_2AR[8] offer a good opportunity to study selective binding using molecular modeling and simulation techniques. A number of computational studies have already explored the binding pocket of β_2AR[9−12] and the conformational properties,[12,13] of the receptor through homology modeling,[9] structure-based modeling,[10,11] and molecular dynamics (MD) simulations.[12,13] However, none of these has directly addressed the aforementioned, and clinically vital, problem of β_1AR/β_2AR selectivity.

Nebivolol is a new and highly selective β_1AR-blocker (currently the most β_1AR-selective agent) with unique endothelial nitric oxide (NO)-mediated vasodilating activity.[14−16] The chemical structure of nebivolol is shown in Figure 2. Nebivolol has four chiral centers and 10 stereoisomers[62] but only two of them have antihypertensive activity: the srrr-nebivolol (also know as d-nebivolol) and the rsss-form (also know as l-

* Corresponding author. E-mail: tomasz.rog@gmail.com (T.R.); karolkaszub@gmail.com (K.K.).
† Tampere University of Technology.
‡ University of Warmia and Mazury.
§ University of Southern Denmark.
∥ Aalto University School of Science and Technology.
⊥ The University of Western Ontario.

10.1021/jp909971f
Published on Web 06/04/2010

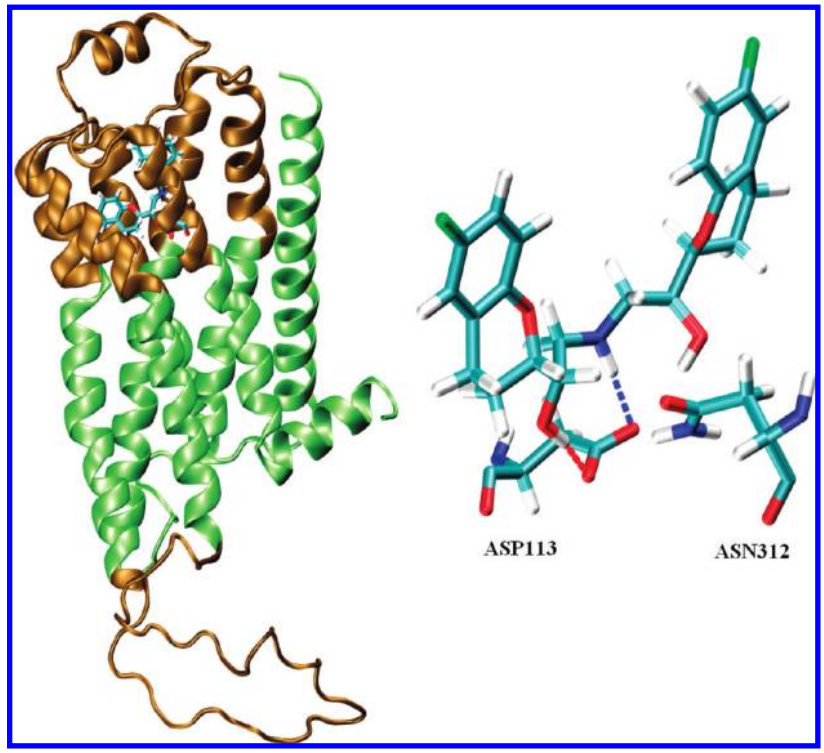

Figure 1. The structure of β_2AR−nebivolol complex after energy minimization (left) and the key H-bonds between ASP113 and nebivolol (right). The binding site area and ICL3 are highlighted in ochre. The protein is shown in the new-cartoon representation, whereas nebivolol and the amino acids ASP 113 and ASN 312 are shown in licorice representation.

nebivolol).[62] Nebivolol does not have many of the common β-blockers' side effects such as fatigue, dizziness, and depression.[14,15] Instead it is characterized by the absence of interactions with other drugs and hence has received attention as a new generation β-blocker.

Despite many pharmacological and clinical studies, we are unaware of any prior computational study of nebivolol. Related atomic-level MD simulations of ligand docking have been performed for other systems such as catechol-O-methyltransfrase[17] and prolyl oligopeptidase.[18] In this paper we combine use of both molecular docking and atomistic classical MD simulations to explore the different binding modes of srrr- and ssss-nebivolol (the least active form of the drug) in the binding site of β_2AR.

Our main findings can be summarized in two parts: First, our simulations indicate that the higher affinity of the srrr-form (and thus its stereoselectivity) originates from energetically favorable interactions with water molecules. To our knowledge, the effect of water as a factor directly influencing binding affinity has been never demonstrated for β-blockers. Second, we identify the amino acids TYR308 and ILE309 in helix 7 and PHE194 in the second extracellular loop (ECL2) along with the corresponding residues in the sequence of β_1AR as presumably influencing the binding selectivity to both of the subtypes. Finally, let us note that here we studied only the binding pocket of β_2AR since related simulations are exceptionally time-consuming. A separate study focusing on the interactions of nebivolol with β_1AR is in progress.

Methods

Molecular Modeling of Third Intracellular (ICL3) Loop of β_2AR. The initial structure of β_2AR (PDB code: 2RH1) was crystallized at 2.4 Å resolution by Cherezov et al.[8] and was obtained from the RCSB Protein Data Bank (PDB) database. Cherezov et al. resolved the structure of β_2AR without the third intracellular loop (ICL3), which they replaced by the stable T4-lysozyme (T4L) fusion protein, thus enabling crystallization. We then had to perform *de novo* modeling of the ICL3 fragment.

The sequence of β_2AR was downloaded from UniProtKB/Swiss-Prot database[19] (access number P07550) and aligned with the X-ray structure of β_2AR. Following the information in the PDB file, the region encompassing the ICL3 was determined to be between amino acids 229 and 267 of the β_2AR sequence (including anchoring residues).

We built 400 models for the ICL3 using MODELER version 9.2[20,21] and its "loopmodel" routine. This method generates an initial loop conformation. A desirable number of loop models was then generated by randomizing the initial loop structure by ±5 Å in each of the Cartesian directions. As the final step, the loop conformations were optimized by MD with simulated annealing.[21] The level of refinement was set to "refine.very_slow" which equaled 15 cycles of MD-simulated annealing. During this, the loop models were heated from the starting temperature of 150 K up to 1300 K and then cooled to 300 K.[21] These models were then ranked using the DOPE-HR method (Discrete Optimized Protein Energy at Higher Resolution), a statistical potential optimized for model assessment. DOPE scoring is designed to select the best structure from a collection of models built by the MODELER software.[21] The best 20 models were selected and evaluated. Due to the presence of "knots" in some the groups of previously selected structures, the model with the best DOPE-HR score and without any structural distortions was considered as the best one and used in docking studies. The full structure of β_2AR obtained through this analysis is shown in Figure 1.

Force-Field Parametrization of Nebivolol. The structures of ssss- and srrr-nebivolol were built and initially minimized using HyperChem software.[22] They were then further geometry-optimized using the Gaussian03 package[23] with the restricted Hartree−Fock (RHF) method and the 6-31G* basis set.

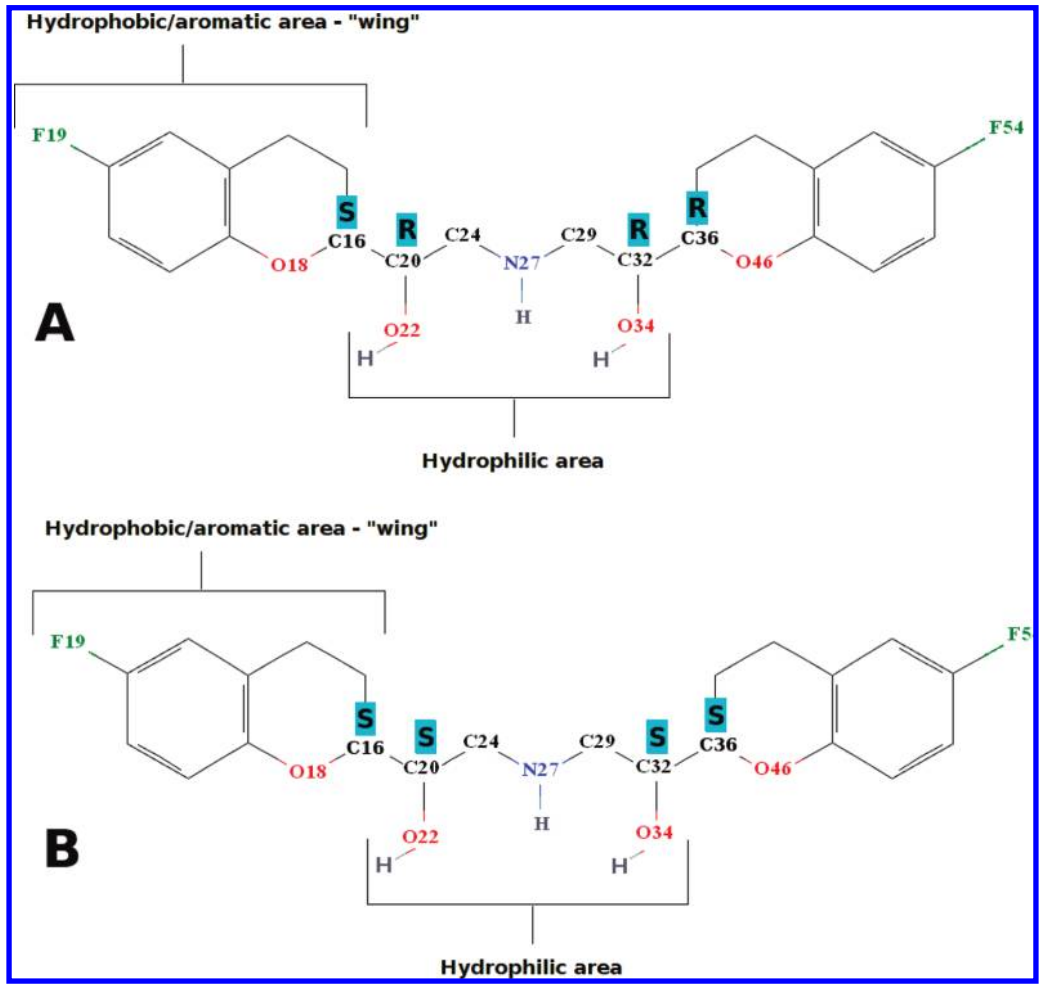

Figure 2. Chemical structure of nebivolol. Color code: oxygen - red, nitrogen - blue, fluorine - green, carbon - black, hydrogen - gray. The simulated structures of the srrr-nebivolol and ssss-nebivolol are shown in panels A and B, respectively. The atoms, which constitute the chiral centers, are labeled by letters S and R.

Frequency calculations at the RHF/6-31G* level were performed to derive the force constants for the missing bonds and angles. Due to the fact that vibrational frequencies from ab initio calculations do not perfectly agree with the corresponding experimental values,[24,25] the scaling factor of 0.9 was applied.[25] Partial atomic charges were determined according to the RESP procedure.[26] Computation of the molecular electrostatic potential (MEP) and charge fitting were done automatically in RESP ESP charge derived (R.E.D.) software version III.[27−29] Finally, the energy of the molecule was minimized by the conjugate gradient method in a CHARMM22 CMAP force-field[30] using NAMD2.6 software.[31]

Molecular Docking of Nebivolol to β_2AR and Subsequent Energy Minimization of Generated Complexes. Nebivolol was docked into the binding site of β_2AR using AutoDock4 and AutoDockTools4[32] software. Docking experiments were performed in this same fashion. The drug was manually placed inside the cavity of β_2AR. The previously derived RESP charges for the ligand (nebivolol) were imported into the AutoGrid module, and the receptor molecule (β_2AR) was embedded into the docking-box. The position of the grid-box, located in the binding pocket of the βAR, corresponded to experimental data.[33,34] The Lamarckian Genetic Algorithm (LGA)[35] was used for docking. The population size was set to 300 individuals, and the number of energy evaluations was set to 50 000 000. Two docking simulations were performed for each stereoisomer. This produced a total of 200 complexes of each ssss- and srrr-nebivolol docked to the binding site of the β_2AR.

The essential features of the binding site of the βAR have been characterized in several experimental studies.[8,34] These show that two amino acids, ASP113 and ASN312, are the key residues for binding. When analyzing the complexes, we focused on obtaining the experimentally observed hydrogen-bonding (H-bonding) patterns between these two essential amino acids and the H-bonding groups of nebivolol (Figure 1). This criterion ensured that the drug compound was properly docked to the active site of β_2AR.

Next, the geometries of the docked complexes were optimized by 15 000 steps using the conjugate gradient method with NAMD2.6 software[31] and the CHARMM22 CMAP force-field.[30] This step was necessary in order to remove possible close contacts between the atoms of the drug compound and those of β_2AR. After geometry optimization, the complexes were ranked according to how well they agreed with the site mutagenesis data.[34] This procedure enabled us to test the combination of NAMD2.6 and CHARMM energy functions as a potentially useful tool for re-evaluation of docked complexes using their minimized energy.

System Preparation. For MD simulations, the *Membrane builder* plug-in of the Visual Molecular Dynamics (VMD) program[36] was used to build a starting structure of a palmitoyl oleoyl phosphatidyl choline (POPC) bilayer. *Membrane builder* builds a slightly disordered POPC membrane. Some disorder was introduced by orienting the lipid acyl chains randomly. This was followed by a short 1 ps equilibration in a vacuum while the lipid chains were left extended. After building the bilayer,

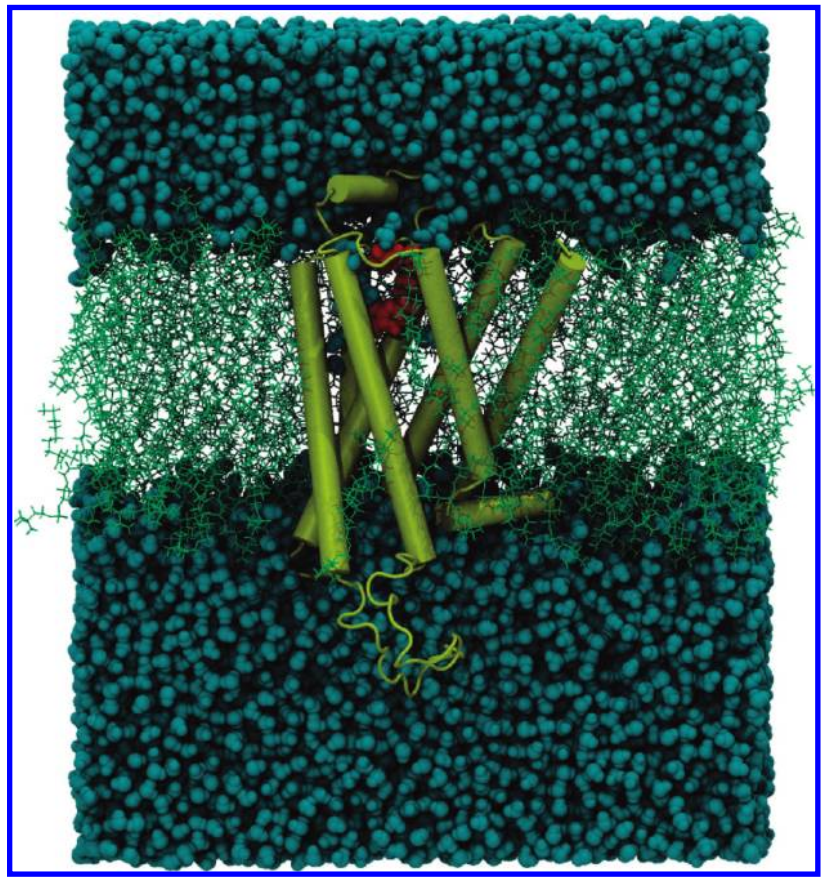

Figure 3. A snapshot showing the β_2AR/ssss-nebivolol/membrane complex at the end of the second simulation. β_2AR is shown in cartoon representation (gold). Nebivolol (red) and water molecules (cyan) are displayed as van der Waals spheres. The POPC molecules (green) surrounding the receptor protein are shown in licorice representation. For clarity, some POPC and water molecules have been removed.

the protein−drug complex was embedded in it and 25 811 TIP3P[37] water molecules were added using the *Solvate* plug-in. After solvating, the system had a rectangular box shape. Overlapping water molecules were removed. To preserve overall charge neutrality, four Cl^- ions[38] were added using the *Autoionize* plug-in. The system dimensions before equilibration were 112 Å × 113 Å × 116 Å. The simulated systems of consisted of 120,828 atoms, including β_2AR protein, 289 POPC molecules, 25 569 water molecules, four Cl^- ions, and the nebivolol compound. An example of the simulated structure of the β_2AR/ssss-nebivolol/membrane complex is shown in Figure 3.

Simulation Parameters. All atomistic MD simulations were performed using the NAMD2.6 package and the CHARMM22 CMAP force field for the protein and CHARMM27,[39−41] for the lipids. Bonded interactions were computed every 1 fs. Short-range nonbonded van der Waals interactions were computed every 2 fs, and the long-range electrostatic ones were computed every 4 fs. Starting from a switching distance of 1 nm, the Lennard-Jones potential was smoothly reduced to zero at a cutoff distance of 1.2 nm. The particle mesh Ewald (PME) algorithm,[42,43] with a grid spacing of 1 Å was used for electrostatics.

The target temperature was 310 K in all simulations. This was controlled using Langevin dynamics[44] with the friction coefficient set to 2.5 ps^{-1}. In NpT simulations (constant pressure, particle number, and temperature), pressure was controlled using the modified Langevin piston Nosé−Hoover method[45−47] with a barostat oscillation coefficient of 100 fs and a damping coefficient of 50 fs. The anisotropic pressure coupling scheme was used in the NpT simulations. Target pressure was 1 atm.

System Equilibration and Production Simulations. Equilibration of the POPC bilayer with the embedded protein−drug complex was performed in two stages. The first involved 5000 steps of energy minimization using the conjugate gradient method. This was followed by a 1 ns MD simulation in the NVT (constant particle number, volume, and temperature) ensemble. This allowed for the hydrophobic core of the POPC bilayer to disorder. All atoms in the simulated system, with the exception of the lipid chains, were restrained to their initial positions with a force constant of 2 kcal/(mol $Å^2$). In the second stage, the system was minimized by 2000 steps using the conjugate gradient method and then simulated for 1 ns in the NpT conditions. The atoms of the protein's backbone were restrained with a force constant of 2 kcal/(mol $Å^2$), while all the other atoms were free to move. This partially equilibrated system was used in the production phase.

The production runs were done in the NPT ensemble. The receptor protein was unconstrained, and the whole complex was allowed to relax. In order to better determine the preferred binding site, three 30 ns simulations of ssss-nebivolol complexed with β_2AR and three 30 ns simulations of srrr-nebivolol bound to β_2AR, were performed. In addition, one 30 ns simulation was performed with the ligand-free (apo-β_2AR) protein. The total simulation time, including relaxation and production runs, was 220 ns.

Results

Docking and Energy Minimization. We performed two parallel docking runs that yielded 200 conformations of each ssss- and srrr-nebivolol complexed with β_2AR. Results were

clustered using 2 Å tolerance. In both of the docking simulations, regardless of the steric configuration of the drug, the most populated clusters showed the same H-bonding pattern. The donor groups of nebivolol were observed to interact with the acceptors located at ASP113 and ASN312. Additionally, one of the fluorine atoms of nebivolol formed H-bonds with residues SER203 and SER204. In conclusion, the obtained H-bonding pattern fully agreed with mutagenesis data describing the essential interactions in the binding cavity of β_2AR.[8,34]

The docked complexes of the ssss/srrr-nebivolol and β_2AR were minimized by 15 000 steps of the conjugate gradient method to remove all possible clashes. We observed that the potential energy function of the CHARMM force-field reranked docked complexes properly. The key H-bonding interaction with ssss-nebivolol was between ASP113 and the amine group of the drug was detected only in the first ranked solution. The minimized energy of that complex was −5548.1 kcal/mol. We assessed that this model agreed best with experimental data as it described the most important interactions in the binding cavity of β_2AR.[34] We used this complex as the structure in the subsequent atomistic MD simulations. The results of docking suggest that srrr-nebivolol was docked slightly better than the ssss-isomer. The interactions involving both ASP113 and ASN312 were present in the second and third complexes. However, only in the second one was the amino acid ASP113 exchanging a proton with the amine group of the drug. This interaction is of essential importance for all βARs.[34] We concluded that complex 2 was the best one, and its structure was used in our MD simulations. The results of energy minimization also showed that the srrr-form interacted much more effectively with β_2AR than the ssss-enantiomer. The minimized energy of the second complex was −5582.5 kcal/mol.

Molecular Dynamics: Stability of Receptor Protein. The structure of β_2AR remained stable in all MD simulations of ssss-nebivolol and srrr-nebivolol. Figure 4 shows the root-mean-square deviation (RMSD) calculated for the protein's backbone atoms excluding the flexible ICL3 loop. The RMSD at time t is defined as

$$\mathrm{RMSD}(t) = \sqrt{\frac{\sum_{i=1}^{N} [\mathrm{r}_i(t) - \mathrm{r}_i(t=0)]^2}{N}}$$

where $r_i(t)$ is the position of the ith particle at time t, and N is the number of particles. RMSD's were calculated using VMD. Conformation of the ligand-free receptor was less dynamic than in nebivolol−β_2AR simulations. In all performed simulations, the most flexible part of the receptor structure was the ICL3 region. Table 1 shows that the secondary structure of β_2AR was preserved in all of the performed simulations. The only noted changes (if any) were related to the residues at C/N-termini of the helices.

Structure of Nebivolol and Time Evolution of Ligand Conformation. The structure of the nebivolol molecule can be divided into two basic parts: hydrophilic and hydrophobic (Figure 2). The hydrophilic part is composed of the C20−C24−N27−C29−C32 sequence and spans two hydrophobic/aromatic parts; we refer to this whole region as "the wings". The hydrophilic region has three H-bonding groups, which function as H-bond donors. These two groups are the hydroxyl groups around oxygens O22 and O34 (bound to carbons C20 and C32, respectively) and the protonated amine group around nitrogen N27.

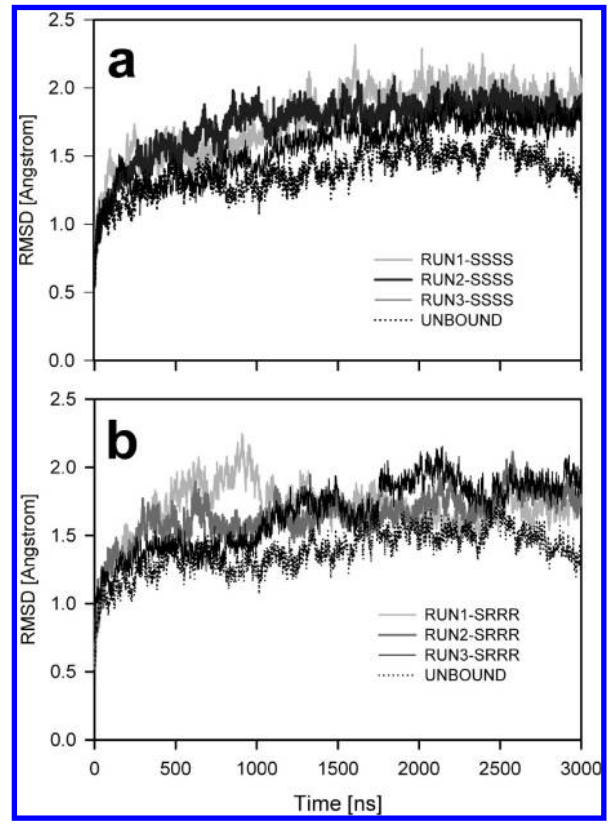

Figure 4. RMSD calculated for the whole receptor excluding ICL3 (residues 229 to 267). Results for ssss-nebviolol are presented in panel a. Structural stability of srrr-nebviolol is shown in panel b.

Conformational changes in the structure of nebivolol were investigated by measuring the distances between its most distant groups, which are the fluorine atoms (Figure 2). The results were visually verified using VMD software.

Our simulations provide an overall qualitative view of nebivolol's behavior in the binding cavity of the β_2AR. The ssss-nebivolol oscillates between the bent and more extended conformations. In all three simulations, the distance between the fluorine atoms was between 13 Å −18 Å and was never less than about 13 Å (see Figure 5). The highly fluctuating structure of the ssss-form favored hydrophobic contacts, mainly with helices 3, 5, 6, and 7. The srrr isomer behaved differently: In all MD runs, the structure of the srrr-form remained in its fully extended configuration (Figure 5). Its structure was very stable (stiff) and no structural changes were observed. This is a major difference in comparison with the highly flexible conformation of the less active ssss-configuration of the drug. The distance between fluorine atoms was always around 19−20 Å (see Figure 5).

Both nebivolol's isomers changed their orientation in the binding site. We observed two different binding modes. The first we called "horizontal". It is characterized by parallel orientation of nebivolol with respect to the bilayer plane (see Figure 6, ssss-run 1). In four simulations (MD run 1,2 for ssss and MD run 1,3 for srrr) nebivolol changed its binding mode to vertical. The vertical binding mode prevented it from interacting with helix 2. In this configuration, the drug was anchored between two distant "walls" of the β_2AR binding site: the first "wall" was formed by helices 3, 4, and 5, while the second one was created by helices 2 and 7. The contact with helix 7 was always much stronger (described in the next section). We also noted that the changes in the binding mode were accompanied by movement of the drug toward ECL2. The srrr-

TABLE 1: The Positions of Helical Fragments after Completed Simulations[a]

structure	ssss-run 1	ssss-run 2	ssss-run 3	srrr-run 1	srrr-run 2	srrr-run 3	unbound	crystal
helix 1	29–60	29–60	29–60	30–60	30–60	31–60	31–60	29–60
helix 2	67–96	67–96	67–96	67–96	67–96	67–96	67–96	67–96
helix 3	103–136	103–135	103–136	103–136	103–136	103–135	103–136	103–136
helix 4	147–170	147–170	147–170	147–170	147–170	147–170	147–170	147–171
helix 5	197–227	197–226	197–228	197–228	197–227	197–229	197–228	197–229
helix 6	267–298	267–298	267–298	267–298	267–298	267–298	267–298	267–298
helix 7	306–328	305–326	305–326	305–328	305–326	305–328	305–326	305–328
helix 8	330–339	330–340	330–339	330–340	330–340	330–340	330–339	330–341
ECL2 helix	179–186	179–184	179–185	179–186	179–185	179–186	179–185	178–187

[a] The secondary structure was calculated using the DSSP (Definition of Secondary Structure of Protein) program.[55]

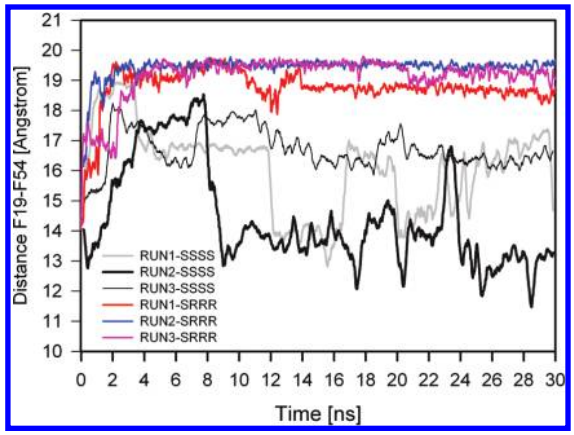

Figure 5. Conformational changes of the nebivolol molecule shown as a function of interatomic distance between fluorine atoms F19 and F54. For clarity, the data were averaged using a running average over a window of 30 data points. The plots made in color correspond to srrr-nebivolol, whereas black coloring scheme shows results for ssss-configuration of the drug.

configuration was less buried in the structure of β_2AR than the ssss-isomer. Thus, the srrr-nebivolol interacted stronger with the ECL2 and others amino acids forming the upper of the binding site.

Binding Site of β_2AR. To understand the exact mode of nebivolol binding to β_2AR, we investigated its conformational properties in the binding site of β_2AR. We mapped the interactions between the different conformations of nebivolol and the receptor. We found a direct relationship between the binding mode of nebivolol's isomers and the existence of specific interactions. We observed clear differences in the binding of ssss and srrr enantiomers. In all simulations, we kept track of the residues within a 3.5 Å radius around the nebivolol molecule that participated in H-bonding (Table 2a,b). We also monitored hydrophobic and aromatic interactions (see Table 3).

Hydrogen Bonds. The existence of an H-bond was defined by the following geometrical criterion:[48] An H-bond was determined to exist if the distance between an acceptor and a donor was ≤3.25 Å and if the angle between the O···O vector and the OH group (the O···O−H angle) was less than 30°. The H-bond analysis was done in the VMD program.

There are only a few polar residues within the cavity region of β_2AR. All of them exhibit 100% sequence conservatism within a whole family of βARs (Supporting Information, Figure 1). This sequence conservatism suggests their critical role in ligand binding. These amino acids are ASP113 (helix 3) and ASN 312 (helix 7). Our analysis confirmed the profound role of these residues. Almost all detected H-bonds related only to ASP113 and ASN312. We also found that heavy atoms of the drug (namely O22, O34, and N27), were responsible of 99% of all detected H-bonds. The H-bonding network between β_2AR and srrr-nebivolol was slightly stronger. Unlike ssss-nebivolol, the receptor protein donated more H-bonds. Thus, compared to ssss-simulations, the lifetime of H-bonding interactions between the drug and the protein was 9 ns longer in the srrr-configuration. In all simulations having ssss-nebivolol docked to the binding site of β_2AR, all H-bonds between drug and protein were systematically distributed between donors O22, O34, and N27. Yet, srrr-nebivolol favored oxygen O22 as the main point of H-bonding interactions. The H-bonds exchanged between protein and donor O22 accounted for 65% of total interaction time.

Water-Mediated H-Bonds and Pocket Hydration. The so-called "water-mediated H-bond" is a special type of H-bonding interaction.[49] In the complexes of ssss-nebivolol and β_2AR, we found 3, 6, and 19 water-mediated H-bonds in MD simulations 1, 2, and 3, respectively. The water bridges between the srrr-form and β_2AR occurred less frequently (Table 2a,b). We also observed an exchange of water molecules during the lifetime of the bond (different water molecules bridged the same donor−acceptor pairs), which resulted in a relatively long interaction time. H-bonds involving ASN312 are a good example of this. Figures 7 and 8 illustrate the extensive hydration of the binding site. This phenomenon was observed for both of nebivolol's isomers. The average numbers of the water molecules for the ssss-form were 16.03, 15.82, and 18.31, respectively in MD runs 1, 2, and 3. For the srrr-form, we observed 16.06 water molecules in the first MD simulation, 18.57 in the second, and 16.36 in the third.

Nonbonded Interactions. To detect hydrophobic interactions between nebivolol and the surrounding amino acids in the cavity of β_2AR, we applied three criteria: First, we identified all residues of β_2AR that appeared throughout the simulation times within a 3.5 Å radius around the nebivolol molecule. Second, we calculated the centers of masses for both nebivolol wings and the protein side chains, and monitored the distances between the centers of masses up to a cutoff distance of 6 Å. Third, the existence of $\pi-\pi$ stacking interactions was verified visually. Nonbonded interactions were analyzed using the VMD program.[36]

Analysis of all six simulations shows that the most common nonbonded interactions involved residues VAL114 (helix 3), VAL117 (helix 3), PHE193 (ECL2) and PHE290 (helix 6) (see Figure 9 and Table 3). The results emphasize the significance of the ECL2 loop, residues PHE193 and PHE194, and in the srrr-simulations also the residue THR195. The two symmetric wings (as defined above) are a characteristic feature of nebivolol. These wings show both aromatic and hydrophobic properties. This reinforces the need for stacking type of interactions between the drug and the protein. We identified $\pi-\pi$ stacking interactions between the side chain of TYR308 and the ssss-form (Figure 9). In most cases, nebivolol, regardless of its steric form,

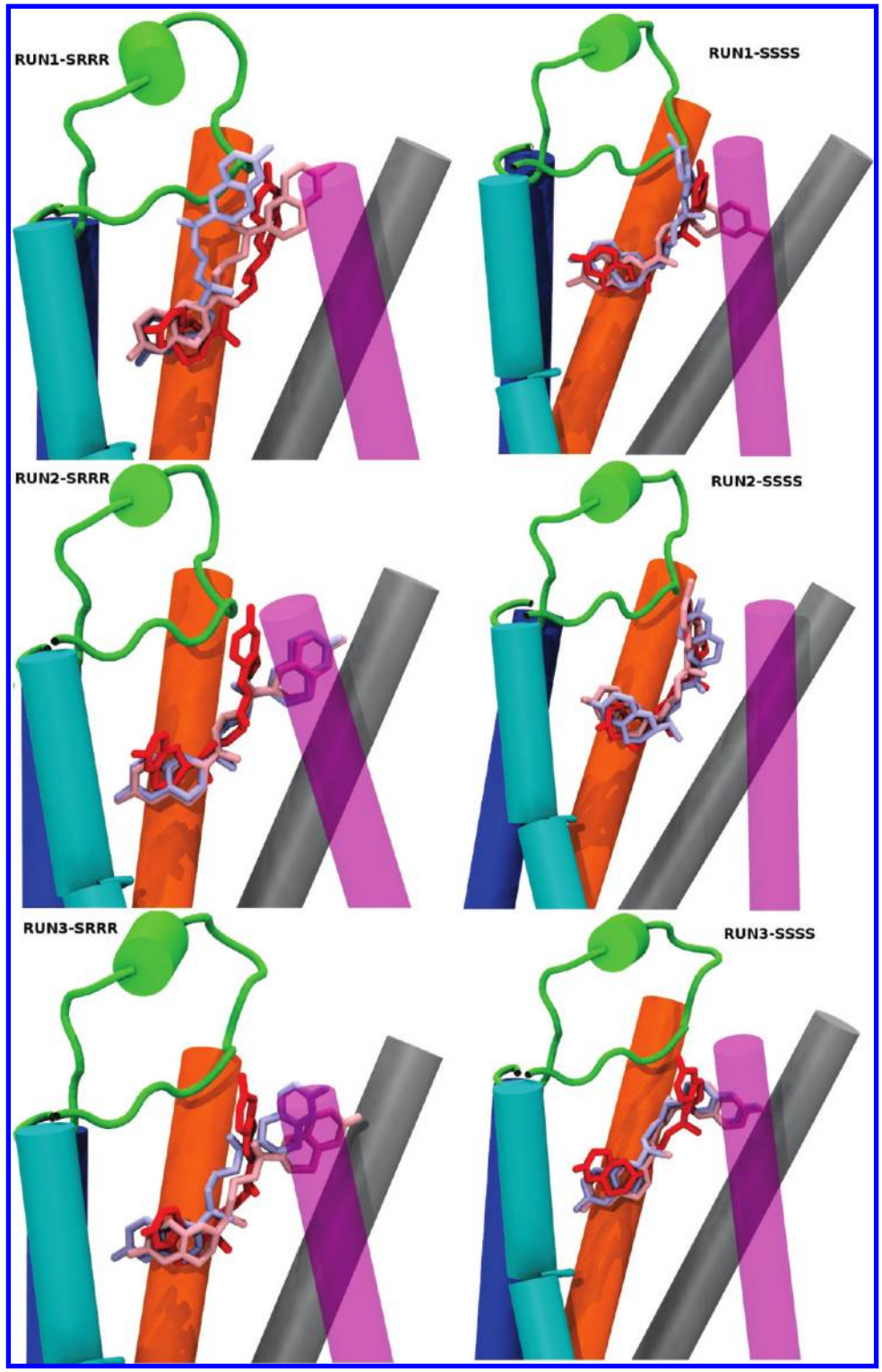

Figure 6. Fluctuations of nebivolol's position in the binding cavity of β_2AR. Helices are shown in the cartoon representation. Color scheme: helix 2 - silver, helix 3 - orange, helix 4 - blue, helix 5 - cyan, helix 7 - magenta (transparent). Nebivolol is displayed using the licorice representation. Its position at 0, 15, and 30 ns is shown in red, gray, and blue, respectively. Helices 1 and 6 were omitted for clarity.

interacted with these same residues but quite often on a different time scale (Table 3). This is related to ILE94 (top of helix 2), THR110, THR118 (helix 3), THR195 (ECL2), TYR199 (h5), PHE289, and TYR308. With the exception of THR110, all residues interacted for a significantly longer time with the srrr-configuration. We concluded that the difference in the interaction time ($\geq$9 ns; 10% of the simulation time) is significant.

As outlined before, two different spatial configurations of nebivolol were simulated. Due to their distinct stereochemical properties, they may interact with β_2AR differently. Thus, it is necessary to introduce an additional criterion to differentiate between the strengths of nonbonded interactions. We decided to apply an energy criterion. The total energy of nonbonded contacts was calculated from the nonbonded parameters listed in the CHARMM force-field. In CHARMM potential, the energy of nonbonded interaction is decomposed into two terms, electrostatic, and van der Waals. The latter one is expressed in the force-field as an effective Lennard-Jones potential. We used

TABLE 2

a. Total Time of Hydrogen Bond Interactions Taking into Account All Three Simulations (90 ns)

ssss-nebivolol

time (ns)	NEB_donor	B_2AR_acceptor	β_2AR_donor	NEB_acceptor	time (ns)
26.31	O34	ASP113 OD1	ASN312 ND2	O34	2.42
18.94	O22	ASN312 OD1	PHE193 N	O18	1.90
11.31	N27	ASP113 OD1	ASN293 ND2	F54	1.28
11.18	N27	ASN 312 OD1	SER 203 OG	F54	0.41
6.61	O34	ASP113 OD2	TRP313 NE1	F19	0.007
4.45	O22	ASP113 OD1	PHE193 N	F19	0.007
1.98	O22	ASP113 OD2	ASN312 ND2	O22	0.006
0.42	N27	ASP113 OD2	ASN312 ND2	O18	0.003
0.003	O22	TYR308 O	ASN312 ND2	N27	0.002
0.003	O22	CYS191 O	LYS305 NZ	F19	0.001
0.001	O34	ASN312 OD1	LYS305 NZ	F19	0.001
			ASN301 ND2	F19	0.001
			ASN293 ND2	O46	0.001

Water-Mediated Hydrogen Bonds

residues bridged		number of water bridges in each simulation			
β_2AR	nebivolol	simulation-1	simulation-2	simulation-3	time (ns)
ASN312 OD1	O34	2		7	16.5
ASN312 OD1	O22		3		2.5
ASN312 ND2	O34			1	4.2
ASN312 ND2	N27			2	1.1
ASP113 OD1	O22	1	2		1.5
THR110 OG1	N27		1		0.8
TYR316 OH	O34			1	8.5
CYS191 O	O22			8	10.9

b. Total Time of Hydrogen Bond Interactions Taking into Account All Three Simulations (90 ns).\

srrr-nebivolol

time (ns)	NEB_donor	β2AR_acceptor	β2AR_donor	NEB_acceptor	time (ns)
31.21	O22	ASP113 OD1	ASN312 NH2	O22	12.56
14.7	O22	ASP113 OD2	THR195 N	O34	5.34
10.31	N27	ASP113 OD1	HIS296 NE2	O46	1.21
9.52	N27	ASP113 OD2	SER207 OG	F19	0.83
8.22	O34	PHE193 O			
6.9	O22	ASN293 OD1			
2.7	O34	ASN312 OD1			

Water-Mediated Hydrogen Bonds

residues bridged		number of water bridges in each simulation			
β2AR	nebivolol	simulation-1	simulation-2	simulation-3	time (ns)
ASP113 OD2	N27	1			4.3
ASN312 OD1	O34	1			1.8
ASN312 ND2	O22			2	4.8
ASN301 OD1	O34		1		2.3
ASN301 OD1	O46		1		1.5
PHE193 O	O34			1	1.26
PHE193 O	O46			1	1
CYS191 O	O46	1			0.5
THR110 OG1	N27	1			1.5

the *namdenergy* program incorporated in the VMD package to extract the total energy of the interaction between nebivolol's enantiomers and the receptor protein.

We observed interesting quantitative differences in the binding energies between the ssss and srrr-forms. The results are listed in Table 4. For both forms, the binding energies were mainly determined by contacts with amino acids TRP109, VAL114, PHE193, PHE194, PHE289, TYR308, and ILE309. They occupy helices 3, 6, 7, and ECL2. We also observed differences in the binding energies for different drug configurations. Residues HIS93, THR118, PHE194, THR195, TYR199, HIS296, and ILE309 interacted more strongly with the srrr-form than with the ssss-form. Table 4 shows that the ssss-form binds slightly more strongly, with a total energy of −34.96 kcal/mol, than its more active srrrr-isomer (overall energy of −33.71 kcal/mol). However, and importantly, these binding energies do not take into account the presence of water in the binding cavity of β_2AR. Figures 7 and 8 demonstrate that water molecules are abundant in the binding site of β_2AR. Thus, we became interested in the contribution of water to the total energy of binding. Water within the 3.5 Å layer between drug and protein was analyzed. The energy of the interaction was computed with

TABLE 3: Total Time of Nonbonded Interactions for ssss-Nebivolol and srrr-Nebivolol

		time (ns)		
structure	residue	neb-ssss	neb-srrr	interaction
helix II	VAL86	9	0	hydrophobic
helix II	GLY90	39	30	hydrophobic
helix II	HIS93	30	30	hydrophobic
helix II	HIS93	0	19	π-STACK
helix II	ILE94	4.0	50	hydrophobic
helix III	TRP109	44	48	hydrophobic
helix III	THR110	42	0	hydrophobic
helix III	VAL114	90	90	hydrophobic
helix III	VAL117	90	90	hydrophobic
helix III	THR118	26	76	hydrophobic
ECL2	PHE193	90	90	hydrophobic
ECL2	PHE194	48	29	hydrophobic
ECL2	THR195	30	90	hydrophobic
helix V	TYR199	48	90	hydrophobic
helix VI	TRP286	30	48	hydrophobic
helix VI	PHE289	60	90	hydrophobic
helix VI	PHE290	90	90	hydrophobic
helix VI	HIS296	0	20	hydrophobic
helix VII	TYR308	0	30	hydrophobic
helix VII	TYR308	23	20	π-STACK
helix VII	ILE309	72	70	hydrophobic
helix VII	TRP313	26	30	hydrophobic
helix VII	TYR316	30	30	hydrophobic

separately calculated energies for water−protein and water−drug interactions. The energies were then averaged and summed to give a total nonbonded energy between water and the protein−drug complex. The results are presented in the bottom part of Table 4. The total energy of the interaction with water was −152.53 and −156.095 kcal/mol for the ssss- and the srrr-configuration, respectively.

Discussion

We performed MD simulations of the β_2AR in the presence and absence of nebivolol. Next, we simulated ssss-nebivolol and srrr-nebivolol,[62] the two distinct nebivolol entantiomers. The srrr-nebivolol binds with relatively high affinity to β_1AR and β_2AR.[60] At the same time, it is highly β_1AR selective, whereas the ssss-form binds with very low affinity to both of the subtypes.[62]

We were interested in determining which residues interact preferably with the srrr-form, as well as those that interact strongly with the ssss-isomer. The results were engaging (see Table 4): we found that the ssss-form interacts more favorably with the deeper area of the binding site of β_2AR (Tables 3 and 4), mainly with residues TRP109, VAL114, THR110, and PHE289. In contrast, the srrr-form is favored in the upper part of the active site.

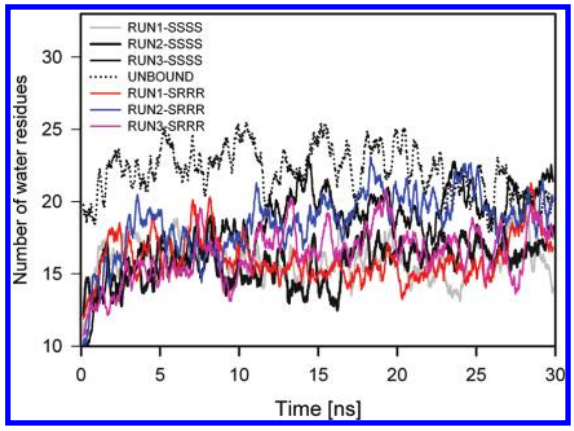

Figure 7. Hydration of the binding pocket. For clarity, data were averaged using a running average over a window of 30 data points.

The above observations can be explained by the different binding modes of the ssss- and srrr-forms. First, the ssss-form was situated deeper inside the binding site of β_2AR than the srrr-form. Second, the results show that both isomers prefer a vertical orientation in the binding site with respect to the bilayer plane. We performed six simulations, and in four of them we observed switching to the "vertical binding mode". Due to its less extended structure, the deeply immersed ssss-nebivolol was unable to interact with the upper part of the binding pocket as effectively as the more extended srrr-configuration.

Once the energies for all residues involved in the interactions were summed up (see Table 4), we found that the ssss-isomer binds with a slightly better energy of −1.25 kcal/mol. The more favorable energy comes mainly from the stronger interactions with TRP109 and PHE193. The binding site of β_2AR has three binding elements: protein, nebivolol, and the water molecules. The high hydration of the binding site drew our attention from the very beginning: In each run, we noticed that there were approximately 16 water molecules between nebivolol and the protein side chains (see Figures 7 and 8). Thus, we decided to clarify the role of water in nebivolol's binding: We calculated the number of water bridges between the protein and the drug and observed more water-mediated H-bonds (Table 2a,b) for the ssss-form. We also noticed that the majority of the water bridges were related to ASP113 and ASN312. We propose that water may be responsible for preserving the required H-bonding pattern between these key residues of the β_2AR cavity and nebivolol. This is particularly true when a drug molecule fluctuates in the pocket. Even a minor change in the position (or/and conformation) of the drug molecule can interrupt the H-bond network.

The number of the H-bonds cannot be the sole decisive criterion defining the configurations that interact more effectively with water. The observed abundance of water molecules in the binding site suggests, however, that they may have a significant contribution to the total energy of binding. We observed this in our simulations: We calculated the energies of the water−drug and water−protein interactions. Next, we added these two components to the previously computed energies for direct protein−drug contacts (see Table 4). A total protein−drug−water interaction energy of −152.53 kcal/mol for the ssss and −156.095 kcal/mol for the srrr-form was obtained. The presence of water in the binding site of β_2AR lowered the binding energy in both simulations regardless of the steric configuration of the drug. Water penetration in the binding site makes the formation of the β_2AR−srrr-nebivolol complex more favorable by −3.565 of kcal/mol. Clearly, our simulations demonstrate that the srrr-form has a more favorable binding energy than its ssss-enantiomer due to its interactions with water molecules. In other words, the experimentally observed[60] higher stereoselectivity of the srrr-form to β_2AR is due to water.

The β_2AR binding site has been investigated in many computational studies including atomistic MD simulations on microsecond time scales.[11,13] One difficulty is that, even when atomistic, docking studies[11] cannot provide information about possible water penetration since docking simulations do not probe the dynamics like MD simulations do. Previous MD simulations suggest low hydration of the binding site and an ionic lock mechanism.[13] They also show, however, that some water molecules reach the interior of β_2AR[13,59] and yet do not

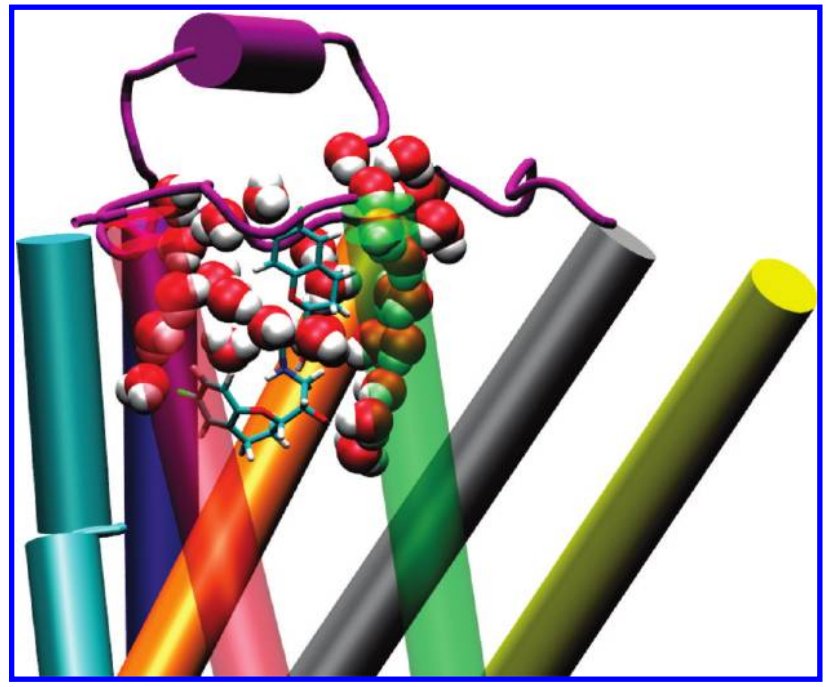

Figure 8. Hydration of the binding pocket. Transmembrane domains of β_2AR are shown in cartoon representation, the coloring pattern as follows: helix 1 - yellow; helix 2 - silver; helix 3 - orange; helix 4 - blue; helix 5 - cyan; helix 6 - red, transparent representation; helix 7 - green, transparent representation. The waters are displayed as van der Waals spheres, oxygen atoms are colored in red, hydrogens are shown in white color. The extracellular loops are colored in magenta. Nebivolol is displayed in licorice representation and its atoms are colored as follows: hydorogens in white, fluorines in green, carbons in cyan, nitrogen in blue, and oxygens in red.

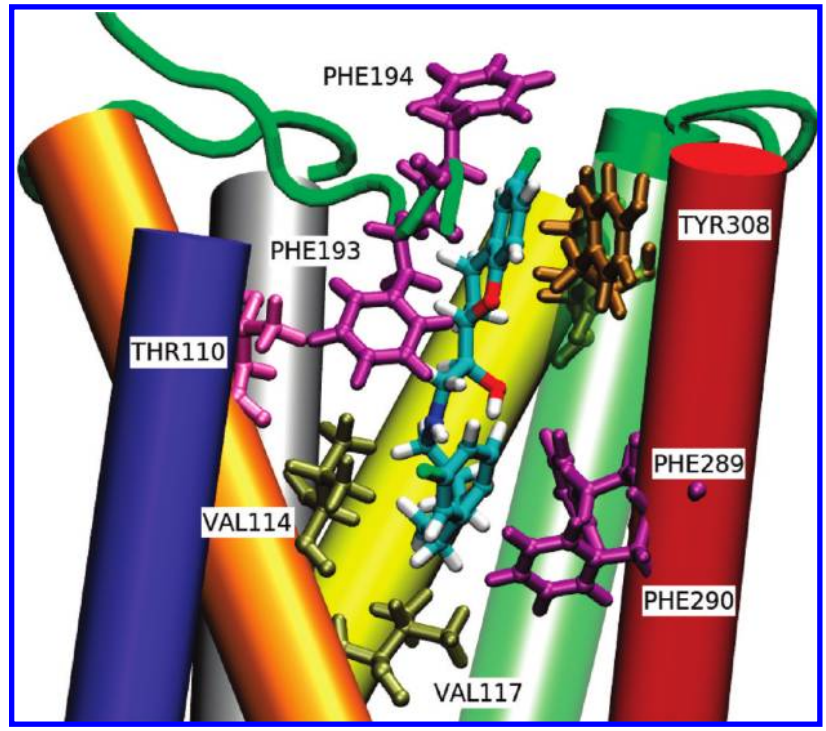

Figure 9. Nonbonded interactions in the binding cavity of β_2AR. Helices are shown in cartoon representation. The color scheme is the same as in Figure 8. Nebivolol and interacting residues are displayed in the CPK representation. Helix 5, amino acid TRP109, ILE309, and part of ECL2 were omitted for clarity.

rule out hydration when a ligand is present. It has been speculated, in connection with experimental studies, that hydration may be an important factor in activating the binding site.[63] Our results strongly suggest that water penetration into the receptor's binding site that is caused by the opened conformation of ECL2 is unavoidable. From this, we can also suggest that water may play an important role in the activation processes of β_2AR[59] and, most likely, in other GPCRs.[64] We observed that some water molecules were able to even go beyond the binding site and reach the interface between the helices or the "nest" between helix turns. This firmly demonstrates that water influences the dynamics and the conformation of β_2AR.

One of the most desired properties of β-blockers is β_1AR selectivity. Ligand selectivity toward β_1AR and β_2AR is a complex problem because aligned amino acid sequences of the aforementioned subtypes show extreme conservatism, especially

TABLE 4: Averaged Energies of Nonbonded interactions for ssss-Nebivolol and srrr-Nebivolol

	average energies [kcal/mol]		
residue	neb-ssss	neb-srrr	energy difference
VAL86	−0.05	−0.01	−0.04
GLY90	−0.12	0.08	−0.05
HIS93	−0.86	−1.41	−0.54
ILE94	−0.49	−0.54	−0.05
TRP109	−3.93	−2.01	−1.92
THR110	−2.27	−0.97	−1.29
VAL114	−4.48	−3.88	−0.6
VAL117	−0.74	−0.36	−0.37
THR118	−0.26	−0.76	−0.5
PHE193	−6.25	−4.76	−1.49
PHE194	−0.8	−1.35	−0.56
THR195	−0.61	−1.73	−1.12
TYR199	−0.92	−1.42	−0.5
TRP286	−0.97	−1.25	−0.27
PHE289	−3.52	−2.98	−0.55
PHE290	−1.47	−1.68	−0.2
HIS296	−0.52	−1.38	−0.87
TYR308	−4.07	−3.59	−0.48
ILE309	−1.41	−2.78	−1.37
TRP313	−1	−0.68	−0.32
TYR316	−0.23	−0.26	−0.04
Total_energy	−34.96	−33.71	−1.25
Binding Energies for Water−Protein and Water−Drug Interactions			
drug−water	−13.16	−13.06	−0.1
protein−water	−104.41	−109.32	−4.911
Summarized Binding Energies for Direct and Water-Mediated Interactions			
	−152.53	−156.095	−3.565

with respect to the residues in the cavity area (Supporting Information, Figure 1). This suggests that subtype-selective binding can be related to residues existing outside the transmembrane cores and are not merely related to those buried deep in the cavity of β_2AR. The results of our simulations, complemented by sequence analysis and available literature data,[50−53] strongly support this hypothesis: First, the multiple sequence alignment (MSA) shows that extracellular ends of helices 2 and 7 and the loops areas, including ECL2 (Supporting Information, Figure 1),[56−58] are the least conservative regions between β_1AR and β_2AR. This alone points to their possible involvement in selectivity. Second, we have simulated two optical isomers of nebviolol, specifically, ssss and srrr. The ssss-form binds with very low affinities to both β_1AR and β_2AR. In contrast, the srrr-configuration is preferred by both subtypes.[60]

Our results suggest that the srrr-form has an energetically more favorable binding mode than the ssss-form and that it interacts more strongly with β_2AR. Despite its β_1AR-selectivity, the srrr-form also binds to β_2AR. This implies that simulations of the srrr-configuration complexed with β_2AR should provide valuable data regarding selectivity. We identified sequentially nonconserved residues situated in the upper region of the β_2AR binding site. These residues may determine selectivity between the two discussed subtypes of βARs. The first two residues, HIS93 and ILE94, occupy the top of helix 2. Amino acid PHE194 is situated in the middle of ECL2, whereas the remaining HIS296, TYR308, and ILE309 are located at the extracellular ends of helices 6 and 7. Interestingly, only the srrr-configuration had additional contacts with HIS93 and HIS296. Both HIS93 and HIS296 have already been mutated,[61] but that work[61] did not address selectivity. Hence, it is impossible to draw any conclusions about how HIS93ALA and HIS296ALA mutants influence binding. The positions occupied by PHE194, THR195, and ILE309 have yet to be mutated. The effect of TYR308A mutation on binding has been documented (see below).

Having no mutational data directly referring to the sequences of β_1AR or β_2AR, our results are discussed here in the context of the mutational studies that have been done for other GPCRs. These works are in line with our simulations and point to helix 7 and ECL2 as "selective regions" of their binding sites. Recent analysis shows that the area of ECL2 plays an essential role in high affinity binding and contributes to ligand selectivity.[50−52] Detailed mutagenesis studies of the human muscarinic receptor M_2 (M_2R) show that amino acids TYR177 (central part of ECL2) and THR423 located at the top of helix 7 largely contribute to the binding selectivity of M_2R/M_5R subtypes.[51] Similar investigations identified ILE183 and ILE184 as a pair of residues that also determine binding and selectivity of different antagonists for human dopamine D_2 receptor (D_2R).[52] We also compared the sequences of β_2AR, M_2, and D_2 receptors. The disulfide linkage between helix 3 and ECL2 is a structural feature conserved by evolution in almost all rhodopsin-like GPCRs.[52] In the M_2 receptor, this disulfide involves CYS96-CYS176, in D_2 it involves residues CYS107-CYS182, and in β_2AR it involves residues CYS190-CYS191. Guided by the disulfide pattern, we aligned the sequences of β_2AR, M_2R, and D_2R (Supporting Information, Figures 2 and 3). The results of this sequence alignment show that PHE194 of β_2AR corresponds to ILE184 of D_2R and equals ILE178 or PHE181 of M_2R. This suggests that PHE194, along with its positional equivalent in β_1AR (namely VAL219), function as a selective epitope.

Regarding the residues of helix 7, we found that TYR308 and ILE309 of β_2AR and the corresponding amino acids of the β_1AR, namely PHE359 and VAL360, might also influence β_1AR/β_2AR subtype selectivities of β-adrenergic antagonists. These findings are again supported by site-directed mutagenesis experiments[54] and the results of sequence alignment in three ways: First, TYR308 equals THR423 in M_2R (Supporting Information, Figures 2 and 3). Second, TYR308 is an essential amino acid for high affinity binding of the β_2AR-selective agonist TA-2005.[54] Third, the binding sites for agonists and antagonists have a partial overlap.[34] Our findings also agree with those of Warne et al.[7] who suggested that the precise position occupied by TYR308 may be a determinant of selectivity for β_1AR/β_2AR subtypes. The second pinpointed residue of helix 7 in β_2AR is ILE309. Interestingly, ILE309 is the immediate neighbor of TYR308 (Supporting Information, Figures 2 and 3) and thus naturally identifies this amino acid as another candidate to be a selective epitope of the β_2AR binding site. The mutation of ILE309 to ALA did not, however, affect the binding of TA-2005 to β_2AR.[54] It could be that the position occupied by ILE309 serves as an antagonist-specific (at least nebivolol-specific) site of interaction. This finding reflects the structural differences between the binding domains for antagonists and agonists in βAR subtypes. As βAR antagonists typically are bulkier than agonists, the binding domains for antagonists are usually larger. The individual structural properties of each compound define unique points of interactions. It is very probable that the binding of nebivolol requires hydrophobic interaction with ILE309, which is not necessarily the case for TA-2005. Thus, ILE309 and VAL360 may also be responsible for selective binding of large β-blocking agents to β_2AR and β_1AR, respectively.

In summary, we have identified five epitopes: HIS93, HIS296, PHE194, TYR308, and ILE309. The results of MSA revealed that PHE194, TYR308, and ILE309 correspond to

residues determining subtype selective binding in other aminergic GPCRs. Since nebivolol is the most β_1AR-selective agent,[14−16] it is probable that these five residues are also involved in the binding of other β_1AR-selective antagonist molecules.

We have investigated the interactions in the binding pocket of β_2AR. We can only speculate about how these amino acids and the corresponding residues of β_1AR determine selectivity of binding toward both subtypes. Hopefully, further simulations performed for the srrr- and ssss-configurations and complexed with β_1AR will provide us with a better understanding of how these residues determine the selectivity of binding toward both of these subtypes.

Conclusions

1. Our results indicate the fundamental role of water in the binding site of β_2AR.

2. Water directly influences the binding affinity of nebivolol's enantiomers and enhances the stereoselectivity of the srrr-form for β_2AR. To our knowledge, the effect of water as a factor of directly influencing the binding affinity has been never demonstrated for β-blockers.

3. Our results are in the line with the experiments of Spijker et al.[59] and Pardo et al.[64] who propose that water can be an important factor influencing the activation process of β_2AR.

4. Despite their stochastic nature, the relatively high number of water-mediated H-bonds, involving mainly ASP113 and ASN312, revealed water as a medium-providing environment for key H-bonding interactions between drug and β_2AR.

5. Our simulations revealed that amino acids PHE194, TYR308, and ILE309 in β_2AR and their positional equivalents in the β_1AR subtype may be important epitopes for β_1AR/β_2AR selectivity of nebivolol.

6. There is no mutational data available for HIS93 and HIS296. Our results do, however, point to these amino acids as possibly being involved in subtype selective binding.

Acknowledgment. We would like to thank the Shared Hierarchical Academic Research Computing Network (SHARCNET: www.sharcnet.ca), the Academic Computer Center (CI TASK) in Gdansk, Poland, and the Finnish IT Centre for Science (CSC) for the computational time. Financial support has been provided by the Natural Sciences and Engineering Research Council of Canada (M.K.) and the Academy of Finland (T.R. and I.V.). The Finnish Graduate School in Computational Sciences is also thanked for support (K.K.).

Supporting Information Available: MSA of all βARs. MSA of β_2AR, M_2, and D_2 receptors. PDB-format coordinates of 10 β_2AR−ssss-nebivolol complexes and 10 complexes of the srrr-nebivolol bound to β_2AR, minimized in CHARMM force-field and sorted according to their energy. This material is available free of charge via the Internet at http://pubs.acs.org.

References and Notes

(1) Frishman, W. H. β-Adrenergic blockers: A 50-year historical perspective. *Am. J. Ther.* **2008**, *15*, 565–576.

(2) Bristow, M. R. β-Adrenergic receptor blockade in chronic heart failure. *Circulation* **2000**, *101*, 558–569.

(3) Taylor, M. R. G. Pharmacogenetics of the human β-adrenergic receptors. *Pharmacogenomics. J.* **2007**, *7*, 29–37.

(4) Lopez-Sendon, J.; Swedberg, K.; McMurray, J.; Tamargo, J.; Maggioni, A. P.; Dargie, H.; Tendera, M.; Waagstein, F.; Kjekshus, J.; Lechat, P.; Torp-Pedersen, C. Expert consensus document on β-adrenergic receptor blockers. *Eur. Heart. J.* **2004**, *25*, 1341–1362.

(5) Westfall, T. C.; Westfall, D. P. Adrenergic agonists and antagonists. In *Goodman and Gilman's The Pharmacological Basis of Therapeutics*, 11th ed. Brunton, L. L.; Lazo, J. S.; Parker, K. L., Eds.; McGraw-Hill: New York, 2006; Chapter 11.

(6) Xiao, R. P.; Zhu, W.; Zheng, M.; Chakir, K.; Bond, R.; Lakatta, E. G.; Cheng, H. Subtype-specific β-adrenoreceptor signaling pathways in the heart and their potential clinical implications. *Trends Pharmacol. Sci.* **2004**, *25*, 358–365.

(7) Warne, T.; Serrano-Vega, M. J.; Baker, J. G.; Moukhametzianov, R.; Edwards, P. C.; Henderson, R.; Leslie, A. G. W.; Tate, C. G.; Schertler, G. F. X. Structure of B_1-adrenergic G-protein-coupled receptor. *Nature* **2008**, *454*, 486–491.

(8) Cherezov, V.; Rosenbaum, D. M.; Hanson, M. A.; Rasmussen, S. G.; Thian, F. S.; Kobilka, T. S.; Choi, H. J.; Kuhn, P.; Weis, W. I.; Kobilka, B. K.; Stevens, R. C. High-resolution crystal structure of an engineered human β2-adrenergic G protein-coupled receptor. *Science* **2007**, *318*, 1258–126.

(9) Chelikani, P.; Hornak, V.; Eilers, M.; Reeves, P. J.; Smith, S. O.; RajBhandary, U. L.; Gobind-Khorana, H. Role of group-conserved residues in the helical core of β2-adrenergic receptor. *Proc. Natl. Acad. Sci. U.S.A.* **2007**, *104*, 7027–7032.

(10) De Graaf, C.; Rognan, D. Selective structure-based virtual screening for full and partial agonists of the β2 adrenergic receptor. *J. Med. Chem.* **2008**, *51*, 4978–4985.

(11) Kolb, P.; Rosenbaum, D. M.; Irwin, J. J.; Fung, J. J.; Kobilka, B. K.; Shoichet, B. K. Structure-based discovery of β_2-adrenergic receptor ligands. *Proc. Natl. Acad. Sci. U.S.A.* **2009**, *106*, 6843–6848.

(12) Huber, T.; Menon, S.; Sakmar, T. P. Structural basis for ligand binding and specificity in adrenergic receptors: Implications for GPCR-targeted drug discovery. *Biochemistry* **2008**, *47*, 11013–11023.

(13) Dror, R. O.; Arlow, D. H.; Borhani, D. W.; Jensen, M.; Piana, S.; Shaw, D. E. Identification of two distinct inactive conformations of the β_2-adrenergic receptor reconciles structural and biochemical observations. *Proc. Natl. Acad. Sci. U.S.A.* **2009**, *106*, 4689–4694.

(14) Prisant, J. Nebivolol: Pharmacologic profile of an ultraselective, vasodilatory β_1-blocker. *Clin. Pharmacol.* **2008**, *48*, 225–239.

(15) Veverka, A.; Nuzum, D. S.; Jolly, J. L. Nebivolol: A third-generation β-adrenergic blocker. *Ann. Pharmacother.* **2006**, *40*, 1353–1360.

(16) Rosei, E. A.; Rizzoni, D. Metabolic profile of nebivolol, a β-adrenoceptor antagonist with unique characteristics. *Drugs* **2007**, *67*, 1097–1107.

(17) Bunker, A.; Männistö, Pt.; St Pierre, J. F.; Róg, T.; Pomorski, P.; Stimson, L.; Karttunen, M. Molecular dynamics simulations of the enzyme catechol-*O*-methyltransferase: Methodological issues. *SAR QSAR Environ. Res.* **2008**, *19*, 179–89.

(18) Kaszuba, K.; Rog, T.; St. Pierre, J. F.; Männistö, P. T.; Karttunen, M.; Bunker, A. Molecular dynamics study of prolyl oligopetidase with inhibitor in binding cavity. *SAR QSAR Environ. Res.* **2009**, *20*, 595–609.

(19) The UniProt Consortium. The universal protein resource (UniProt) 2009. *Nucleic Acids Res.* **2009**, *37*, D169−D174.

(20) Sali, A.; Blundell, T. L. Comparative protein modelling by satisfaction of spatial restraints. *J. Mol. Biol.* **1993**, *234*, 779–815.

(21) Sali, A.; Webb, B.; Madhusudhan, M. S.; Shen M.-Y.; Marti-Renom, M. A.; Eswar, N.; Alber, F.; Topf, M.; Oliva, B.; Fiser, A.; Sanchez, R.; Yerkovich, B.; Badretdinov, A.; Melo, F.; Overington, J. P.; Feyfant, E. *MODELLER, A Program for Protein Structure Modeling*, release 9v2, r5542; University of California, San Francisco: San Francisco, CA, 2007.

(22) Coleman, W. F.; Arumainayagam, C. R. HyperChem 5 (by Hypercube, Inc.). *J. Chem. Educ.* **1998**, *75*, 416.

(23) Frisch, M. J.; Trucks, G. W.; Schlegel, H. B.; Scuseria, G. E.; Robb, M. A.; Cheeseman, J. R.; Montgomery, Jr., J. A.; Vreven, T.; Kudin, K. N.; Burant, J. C.; Millam, J. M.; Iyengar, S. S.; Tomasi, J.; Barone, V.; Mennucci, B.; Cossi, M.; Scalmani, G.; Rega, N.; Petersson, G. A.; Nakatsuji, H.; Hada, M.; Ehara, M.; Toyota, K.; Fukuda, R.; Hasegawa, J.; Ishida, M.; Nakajima, T.; Honda, Y.; Kitao, O.; Nakai, H.; Klene, M.; Li, X.; Knox, J. E.; Hratchian, H. P.; Cross, J. B.; Bakken, V.; Adamo, C.; Jaramillo, J.; Gomperts, R.; Stratmann, R. E.; Yazyev, O.; Austin, A. J.; Cammi, R.; Pomelli, C.; Ochterski, J. W.; Ayala, P. Y.; Morokuma, K.; Voth, G. A.; Salvador, P.; Dannenberg, J. J.; Zakrzewski, V. G.; Dapprich, S.; Daniels, A. D.; Strain, M. C.; Farkas, O.; Malick, D. K.; Rabuck, A. D.; Raghavachari, K.; Foresman, J. B.; Ortiz, J. V.; Cui, Q.; Baboul, A. G.; Clifford, S.; Cioslowski, J.; Stefanov, B. B.; Liu, G.; Liashenko, A.; Piskorz, P.; Komaromi, I.; Martin, R. L.; Fox, D. J.; Keith, T.; Al-Laham, M. A.; Peng, C. Y.; Nanayakkara, A.; Challacombe, M.; Gill, P. M. W.; Johnson, B.; Chen, W.; Wong, M. W.; Gonzalez, C.; Pople, J. A.; *Gaussian 03*, revision C.02, Gaussian, Inc.: Wallingford, CT, 2004.

(24) Irikura, K. K.; Johnson, R. D.; Kacker, R. N. Uncertainties in scaling factors for ab initio vibrational frequencies. *J. Phys. Chem.* **2005**, *109*, 8430–8437.

(25) Florian, J.; Johnson, B. G. Comparison and scaling of Hartree−Fock and density functional harmonic force fields. 1. Formamide monomer. *J. Phys. Chem.* **1994**, *98*, 3681–3687.

(26) Bayly, C. I.; Cieplak, P.; Cornell, W.; Kollman, P. A. A well-behaved electrostatic potential based method using charge restraints for deriving atomic charges: The RESP model. *J. Phys. Chem.* **1993**, *97*, 10269–10280.

(27) Pigache, A.; Cieplak, P. F.; Dupradeau, Y. Automatic and highly reproducible RESP and ESP charge derivation: Application to the development of programs RED and X RED. *227th ACS National Meeting*, Anaheim, CA, March 28−April 1, 2004.

(28) Cezard, C.; Vanquelef, E.; Pecher, J.; Sonnet, P.; Cieplak, P.; Derat, E.; Dupradeau, F. Y. RESP charge derivation and force field topology database generation for complex bio-molecular systems and analogs. *236th ACS National Meeting*, Philadelphia, PA, August 17−August 21, 2008.

(29) Cieplak, P.; Dupradeau, F. Y. Including polarization effects in the RESP charge derivation method. *236th ACS National Meeting*, Philadelphia, PA, August 17−August 21, 2008.

(30) Mackerell, A. D.; Feig, M.; Brooks, C. L. Extending the treatment of backbone energetics in protein force fields: Limitations of gas-phase quantum mechanics in reproducing protein conformational distributions in molecular dynamics simulations. *J. Comput. Chem.* **2004**, *25*, 1400–1415.

(31) Phillips, J. C.; Braun, R.; Wang, W.; Gumbart, J.; Tajkhorshid, E.; Villa, E.; Chipot, C.; Skeel, R. D.; Kalé, L.; Schulten, K. Scalable molecular dynamics with NAMD. *J. Comput. Chem.* **2005**, *26*, 1781–1802.

(32) Morris, G. M.; Huey, R.; Lindstrom, W.; Sanner, M. F.; Belew, R. K.; Goodsell, D. S.; Olson, A. J. AutoDock4 and AutoDockTools4: Automated docking with selective receptor flexibility. *J. Comput. Chem.* **2009**, *30*, 2785–2791.

(33) Tota, M. R.; Strader, C. D. Characterization of the binding domain of the β-adrenergic receptor with the fluorescent antagonist carazolol. Evidence for a buried ligand binding site. *J. Biol. Chem.* **1990**, *265*, 16891–16897.

(34) Nagatomo, T.; Ohnuki, T.; Ishiguro, M.; Ahmed, M.; Nakamura, T. β-Adrenoceptors: Three-dimensional structures and binding sites for ligands. *Jpn. J. Pharmacol.* **2001**, *87*, 7–13.

(35) Morris, G. M.; Goodsell, D. S.; Halliday, R. S.; Huey, R.; Hart, W. E.; Belew, R. K.; Olson, A. J. Automated docking using a Lamarckian genetic algorithm and an empirical binding free energy function. *J. Comput. Chem.* **1999**, *19*, 1639–1662.

(36) Humphrey, W.; Dalke, A.; Schulten, K. VMD - Visual molecular dynamics. *J. Mol. Graphics* **1996**, *14*, 33–38.

(37) Jorgensen, W. L.; Chandrasekhar, J.; Madura, J. D.; Impey, R. W.; Klein, M. L. Comparison of simple potential functions for simulating liquid water. *J. Chem. Phys.* **1983**, *79*, 926–935.

(38) Beglov, D.; Roux, B. Finite representation of an infinite bulk system: Solvent boundary potential for computer simulations. *J. Chem. Phys.* **1994**, *100*, 9050–9063.

(39) Feller, S. E.; Gawrisch, G.; MacKerell, A. D. Polyunsaturated fatty acids in lipid bilayers: Intrinsic and environmental contributions to their unique physical properties. *J. Am. Chem. Soc.* **2002**, *124*, 318–326.

(40) Feller, S.; MacKerell, A. D. An improved empirical potential energy function for molecular simulations of phospholipids. *J. Phys. Chem. B* **2000**, *104*, 7510–7515.

(41) Schlenkrich, M.; Brickmann, J.; MacKerell, A. D.; Karplus, M. Empirical potential energy function for phospholipids: Criteria for parameter optimization and applications. In: *Biological Membranes: A Molecular Perspective from Computation and Experiment*; Merz, K. M., Roux, B., Eds.; Birkhauser: Boston, 1996; pp 31−81.

(42) Essman, U.; Perera, L.; Berkowitz, M. L.; Darden, T.; Lee, H.; Pedersen, L. G. A smooth particle mesh Ewald method. *J. Chem. Phys.* **1995**, *103*, 8577–8592.

(43) Karttunen, M.; Rottler, J.; Vattulainen, I.; Sagui, C. Electrostatics in biomolecular simulations: Where are we now and where are we heading? *Curr. Top. Membr.* **2008**, *60*, 49−89.

(44) Grest, G. S.; Kremer, K. Molecular dynamics simulation for polymers in the presence of a heat bath. *Phys. Rev. A* **1986**, *33*, 3628–3631.

(45) Feller, S. E.; Zhang, Y.; Pastor, R. W.; Brooks, B. R. Constant pressure molecular dynamics simulation. The Langevin piston method. *J. Chem. Phys.* **1995**, 103.

(46) Nosé, S. A molecular dynamics method for simulations in the canonical ensemble. *Mol. Phys.* **1984**, *52*, 255–268.

(47) Hoover, W. G. Canonical dynamics: Equilibrium phase-space distributions. *Phys. Rev. A* **1985**, *31*, 1695–1697.

(48) Murzyn, K.; Róg, T.; Jezierski, G.; Kitamura, K.; Pasenkiewicz-Gierula, M. Effects of phospholipid unsaturation on the membrane/water interface: A molecular simulation study. *Biophys. J.* **2001**, *81*, 170–183.

(49) Pasenkiewicz-Gierula, M.; Róg, T.; Kitamura, K.; Kusumi, A. Cholesterol effects on the phosphatidylcholine bilayer polar region: A molecular simulation study. *Biophys. J.* **2000**, *78*, 1376–1389.

(50) Avlani, V. A.; Gregory, K. J.; Morton, C. J.; Parker, M. W.; Sexton, P. M.; Christopoulos, A. Critical role for the second extracellular loop in the binding of both orthosteric and allosteric G protein-coupled receptor ligands. *J. Biol. Chem.* **2007**, *282*, 25677–25686.

(51) Voigtländer, U.; Jöhren, K.; Mohr, M.; Raasch, A.; Tränkle, C.; Buller, S.; Ellis, J.; Höltje, H. D.; Mohr, K. Allosteric site on muscarinic acetylcholine receptors: Identification of two amino acids in the muscarinic M2 receptor that account entirely for the M2/M5 subtype selectivities of some structurally diverse allosteric ligands in *N*-methylscopolamine-occupied receptors. *Mol. Pharmacol.* **2003**, *64*, 21–31.

(52) Shi, L.; Javitch, J. A. The second extracellular loop of the dopamine D2 receptor lines the binding-site crevice. *Proc. Natl. Acad. Sci. U.S.A.* **2004**, *101*, 440–445.

(53) Noda, K.; Saad, Y.; Graham, R. M.; Karnik, S. S. The high affinity state of the β_2-adrenergic receptor requires unique interaction between conserved and non-conserved extracellular loop cysteines. *J. Biol. Chem.* **1994**, *269*, 6743–6752.

(54) Kikkawa, H.; Isogaya, M.; Nagao, T.; Kurose, H. The role of the seventh transmembrane region in high affinity binding of a b2-selective agonist TA-2005. *Mol. Pharmacol.* **1998**, *53*, 128–134.

(55) Kabsch, W.; Sander, C. Definition of secondary structure of protein given a set of 3D coordinates. *Biopolymers* **1983**, *22*, 2577–2637.

(56) Altschul, S. F.; Madden, T. L.; Schäffer, A. A.; Zhang, J.; Zhang, Z.; Miller, W.; Lipman, D. J. Gapped BLAST and PSI-BLAST: A new generation of protein database search programs. *Nucleic Acids Res.* **1997**, *25*, 3389–3402.

(57) Edgar, R. C. MUSCLE: multiple sequence alignment with high accuracy and high throughput. *Nucleic Acids Res.* **2004**, *32*, 1792–97.

(58) Waterhouse, A. M.; Procter, J. B.; Martin, D. M. A.; Clamp, M.; Barton1, G. J. Jalview Version 2−A multiple sequence alignment editor and analysis workbench. *Bioinformatics* **2009**, *25*, 1189–1191.

(59) Spijker, P.; Vaidehi, N.; Freddolino, P. L.; Hilbers, P. A. J.; Goddard, W. A. Dynamic behavior of fully solvated β2-adrenergic receptor, embedded in the membrane with bound agonist or antagonist. *Proc. Natl. Acad. Sci. U.S.A.* **2006**, *103*, 4882–4887.

(60) Bundkirchen, A.; Nguyena, Q.; Brixius, K.; Bolck, B.; Mehlhorn, U.; Schwinger, R. H. G. Lack of inverse agonistic activity of nebivolol, its D- and L-enantiomers and of in vivo metabolized nebivolol in human myocardium. *Eur. J. Pharmacol.* **2003**, *476*, 97–105.

(61) Swaminath, G.; Lee, T. W.; Kobilka, B. Identification of an Allosteric Binding Site for Zn2+ on the β_2 Adrenergic Receptor. *J. Biol. Chem.* **2003**, *278*, 352–356.

(62) Siebert, C. D.; Hansicke, A.; Nagel, T. Stereochemical comparison of nebivolol with other β-blockers. *Chirality* **2008**, *20*, 103–109.

(63) Soriano-Ursúa, M. A.; Trujillo-Ferrara, J. G.; Correa-Basurto, J. J. Scope and difficulty in generating theoretical insights regarding ligand recognition and activation of the β2 adrenergic receptor. *J. Med. Chem.* **2010**, *53*, 923–932.

(64) Pardo, L.; Deupi, X.; Dölker, N.; López-Rodríguez, M. L.; Campillo, M. The role of internal water molecules in the structure and function of the rhodopsin family of G protein-coupled receptors. *ChemBioChem* **2007**, *8*, 19–24.

JP909971F